

# PCCP

Accepted Manuscript



This is an *Accepted Manuscript*, which has been through the Royal Society of Chemistry peer review process and has been accepted for publication.

*Accepted Manuscripts* are published online shortly after acceptance, before technical editing, formatting and proof reading. Using this free service, authors can make their results available to the community, in citable form, before we publish the edited article. We will replace this *Accepted Manuscript* with the edited and formatted *Advance Article* as soon as it is available.

You can find more information about *Accepted Manuscripts* in the [Information for Authors](#).

Please note that technical editing may introduce minor changes to the text and/or graphics, which may alter content. The journal's standard [Terms & Conditions](#) and the [Ethical guidelines](#) still apply. In no event shall the Royal Society of Chemistry be held responsible for any errors or omissions in this *Accepted Manuscript* or any consequences arising from the use of any information it contains.

Cite this: DOI: 10.1039/x0xx00000x

# The driving forces for twisted or planar intramolecular charge transfer

Received 00th January 2012,  
Accepted 00th January 2012Cheng Zhong <sup>a</sup>,

DOI: 10.1039/x0xx00000x

[www.rsc.org/](http://www.rsc.org/)

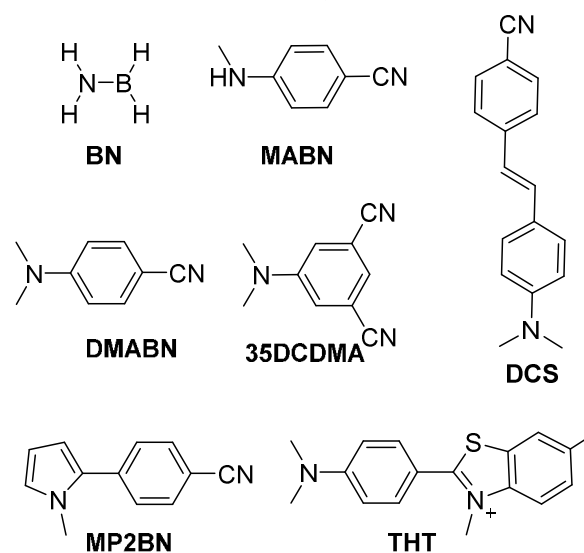
A D-A (donor-acceptor)-type chromophore may twist or flatten in its excited state to form a TICT (twisted intramolecular charge transfer) state or a PICT (planar intramolecular charge transfer) state, respectively. What is the driving force behind this twisting or planarization? Which geometry will occur for a certain D-A chromophore? To answer these questions, both fragment orbital interaction and excited state energy decomposition analyses were performed on several classical TICT/PICT molecules. Three driving forces were identified, namely, energy gap, hole-electron interactions, and excited state relaxation. The contributions of these driving forces in various types of molecules were analyzed to determine how molecular structure affects them. The energy gap difference between the twisted and planar geometries was found to play a decisive role in most situations. Thus, evaluating the frontier orbital interactions between the donor and acceptor effectively predicts whether chromophores planarize or twist in the excited state.

## Introduction

The excited state of D-A (donor-acceptor)-type chromophores undergoes a geometry relaxation that can affect excited state properties. Of the various geometry changes that can occur, rotation around the bond connecting the D and A groups is of particular interest because it usually has the most prominent effect on excited state properties. Two models have been proposed for this change of geometry. The twisted intramolecular charge transfer (TICT) model was proposed by Grabowski to explain the dual fluorescence of **DMABN** (4-(dimethylamino)benzonitrile) and has been confirmed by numerous studies<sup>1-12</sup>. This model states that the D and A groups twist to adopt a perpendicular orientation in the excited state. The resulting orbital decoupling and complete charge transfer are indicated by the red-shifted and weakened fluorescence. In contrast, the PICT (Planar ICT) model proposed by Zachariasse<sup>13-23</sup> and the MICT (Mesomeric ICT) model proposed by Rettig<sup>24-26</sup> state that the D and A groups have a stronger tendency to conjugate with each other in the excited state, as is observed for many D-A type molecules. The dihedral angle between the D and A is smaller (if they are already twisted in the ground state due to steric interactions) and the D-A bond is shorter in the excited state. The corresponding small hole-electron separation and thus small dipole moment are evidenced by the fluorescence having a relatively small Stokes shift and elevated intensity. Because these two geometry changes have opposite effects on excited state properties, predicting the excited state geometry change of an arbitrary D-A molecule is important. Despite the extensive study of the TICT/MICT mechanism, only a few studies have

addressed this question<sup>24, 27-31</sup>, and no clear answer has yet been obtained.

Scheme 1. Molecules examined in this study



To answer this question, the driving forces that twist or flatten the excited state geometry and the structural features that influence those forces must be clarified. The generally accepted driving force for TICT is dipolar solute-solvent interactions, which suggests that the TICT state is stabilized more by a polar solvent than a nonpolar one because it has a larger dipole moment than its counterpart. This theory has abundant experimental support; for **DMABN** and many of its analogues, TICT-type fluorescence diminishes in nonpolar solvents.

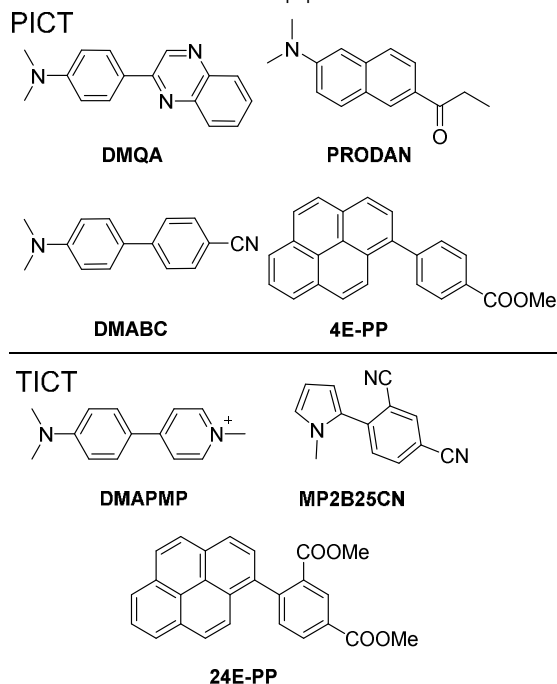
However, only different solvents for the same fluorophore were compared. If different fluorophores were compared, that is, if we wanted to predict whether a specific molecule would exhibit a TICT or PICT state, we would not be able to. The above-described theory implies that a molecule with a large difference in dipole moments between the PICT and TICT states is highly likely to twist in a polar solvent, which indicates that strong D-A pairs (suggests high extent of charge transfer) or large D-A distances (suggests large CT distances) favor the TICT state. In reality, strong D-A pairs do not always undergo TICT, as demonstrated by the comparison between **DMABN** and **35DCDMA** (see scheme 1 for their molecular structures); the latter has a stronger acceptor but shows no sign of TICT fluorescence. In addition, elongating the acceptor usually inhibits TICT formation, as demonstrated for **DCS**<sup>32, 33</sup> (in scheme 1), **DMQA**<sup>34</sup>, **DMABC**<sup>28</sup>, **PRODAN**<sup>35</sup> (in scheme 2), and many other molecules<sup>36, 37</sup>. These molecules were proven to not have a TICT state. The classical review of Grabowski and Rettig<sup>3</sup> noted that the TICT state is more likely to be found in small/short molecules, which cannot be explained by dipolar solute-solvent interactions:

“On the basis of the present stage of knowledge, the TICT model seems to be especially applicable to less extended molecular systems (preferentially with only one aromatic ring).”

The review also noted that no other adequate theory for predicting or explaining the twist angle change direction exists:

“For the majority of the D-A compounds with large aromatic subunits, one can conclude that the internal twisting relaxation in the excited state occurs, if any, either toward larger or toward smaller twist angles, with respect to the conformation in the ground state. Prediction of the direction of change of the twist angle is still far from precise.”

**Scheme 2.** Molecules referenced in this paper



Therefore, there must be other driving forces that dictate the excited state geometry of the D-A molecule. To elaborate these driving forces in association with molecular structure, qualitative orbital interaction diagram and quantitative energy decomposition analyses were performed in this study for several classical TICT/PICT molecules.

## Model and Computational Details

### Excited state energy decomposition

Whether the PICT or TICT state is more stable is determined by their energy. The first excited state energy can be decomposed intuitively as follows:

$$E_{S1} = E_G + E_{gap} + E_{he} + E_R \quad 1$$

$E_{S1}$  is the relaxed first excited state energy.  $E_G$  is the ground state energy obtained via a simple optimization at the CAM-B3LYP/6-311+g(2d,p) level.  $E_{gap}$  is the HOMO-LUMO gap at ground state geometry.  $E_{he}$  is the energy of the hole and electron interactions, which is obtained by subtracting the HOMO-LUMO gap,  $E_{gap}$ , from the excitation energy calculated at the TD-CAM-B3LYP/6-311+g(2d,p) level at the ground state geometry.  $E_R$  is the relaxation energy of the excited state (energy difference between the Frank-Condon and relaxed excited states). The energy of the relaxed excited state is obtained by optimizing the excited state at the TD-CAM-B3LYP/6-311+g(2d,p) level. A geometric constraint on the dihedral angle between the donor and acceptor is applied to obtain a twisted conformation when the planar conformation is more stable.

Subtracting the PICT state energy from the TICT state energy using eq 1 yields the following:

$$\Delta E_{S1}^{T-P} = \Delta E_G^{T-P} + \Delta E_{gap}^{T-P} + \Delta E_{he}^{T-P} + \Delta E_R^{T-P} \quad 2$$

$\Delta E_G^{T-P}$  is the ground state energy difference. This term is always positive because the planar conformation is always more stable in the ground state.  $\Delta E_{S1}^{T-P}$  can indicate which excited state is more stable. Three different situations can be identified. First, a negative  $\Delta E_{S1}^{T-P}$  value means the twisted conformation is more stable for the excited state, and hence, the TICT state is favored. Second, a positive  $\Delta E_{S1}^{T-P}$  greater than  $\Delta E_G^{T-P}$  indicates that the D and A tend to planarize in the excited state, which suggests that the PICT state is favored. Third, a positive  $\Delta E_{S1}^{T-P}$  less than  $\Delta E_G^{T-P}$  indicates that the D and A are less likely to planarize than in the ground state. This state is herein referred to as a PTICT state (Pre-TICT) for convenience. If the ground state is planar because there is no steric repulsion between the D and A groups, the PTICT state behaves like the PICT state because a positive  $\Delta E_{S1}^{T-P}$  ensures that the excited state remains planar. In contrast, if the steric repulsion between the D and A groups creates a twisted ground state, an increased dihedral angle is predicted for the excited state. In this situation, the PTICT state behaves more similarly to a TICT state.

The force of twisting or planarizing should be determined using the four terms on the right side of eq 2. We calculated these four terms separately to determine which contributed the

most, and more importantly, to analyze how structural features influenced these terms.

The energy gap,  $E_{gap}$ , is simply the gap between the HOMO and LUMO. This is based on the assumption that the excitation is dominated by the HOMO to LUMO transition. If the contribution of other orbitals can't be neglect, the error introduced by this simplification will transfer to the  $E_{he}$  term and make it larger. See ESI for detailed discussion.

The hole and electron interaction term,  $E_{he}$ , can be explained as follows:

$$E_{he} \sim K_{he} - J_{he} \quad 3$$

$K_{he}$  is the exchange and correlation repulsion between holes and electrons. This term, which is proportional to the hole-electron spatial overlap, increases the excited state energy.  $J_{he}$  is the Coulomb attraction between holes and electrons. This term decreases the excited state energy and is inversely proportional to the hole-electron distance. The relationship of hole, electron, and exciton has been reviewed by Gregory D. Scholes<sup>38</sup> (further discussion of these terms is provided in the ESI).

The two factors that most affect the  $\Delta E_{he}^{T-P}$  term in eq 2, namely, the hole-electron overlap in a planar state  $O_{he}$  and the reciprocal of the hole-electron distance in a twisting state  $D_{he}^{-1}$ , were quantified using the Multiwfn 3.3.2 program<sup>39</sup> (the definition of these terms is in the ESI). A large  $O_{he}^P$  increases the exchange-correlation repulsion in the planar excited state, whereas no such term existed in the twisted state because of the complete HOMO-LUMO separation. Therefore, a large  $O_{he}^P$  leads to a highly negative  $\Delta E_{he}^{T-P}$  term (favoring the TICT state). A large  $1/D_{he}^T$  indicates a small hole-electron distance and increases the in the TICT state, which facilitates TICT state formation and thus a highly negative  $\Delta E_{he}^{T-P}$  term.

### Fragment orbital interaction diagram

Fragment orbital interaction diagrams can clarify how the D and A orbitals interact with each other to form a complete molecular orbital and how this interaction influences the excited state geometry. The D and A fragments were captured separately from the optimized ground state geometry of the D-A molecule. The bridge atom was capped with hydrogen. A single point calculation of each fragment was then performed to obtain the fragments' orbitals. Using the coefficients for the  $\pi$  orbitals of the D and A fragments and the D-A molecule, a linear regression was performed to obtain the coefficients for each  $\pi$  orbital fragment throughout the entire molecular  $\pi$  orbital. All of these calculations were performed at the CAM-B3LYP/6-311+G(2d,p) level using the Gaussian 09 program.<sup>40</sup>

## Results and Discussion

### I. BN, the simplest TICT molecule

The first case studied is the simplest TICT molecule, boranamine (BN). This molecule serves as an example to illustrate how to analyze TICT/PICT driving forces. For this and subsequent cases, two-level analyses are performed: a

qualitative analysis based on the molecular orbital interaction diagram and a more quantitative analysis based on the energy decomposition diagram. These two analyses are mutually confirming and provide valuable insight.

The orbital interaction diagram for BN is shown in Figure 1. In the ground state, the filled nitrogen p orbital interacts with the empty boron p orbital to form a bonding  $\pi$  orbital and an antibonding  $\pi^*$  orbital. The two nitrogen p-electrons now partially transfer to the boron atom via the bonding  $\pi$  orbital, which is distributed across both atoms, with the minor portion on boron. We classify this molecule as pD-pA (p donor-p acceptor) because both the donor and acceptor only have a p orbital to form conjugation. The reason for this classification is explained later. The energy difference between the nitrogen p orbital and the bonding  $\pi$  orbital is considered the planarization stabilization energy in the ground state. In the excited states, when an electron transfers from  $\pi$  to  $\pi^*$ , the twisted conformation becomes more stable because the destabilizing energy of the electron in the antibonding orbital surpasses the stabilizing energy of the electron in the bonding orbital.

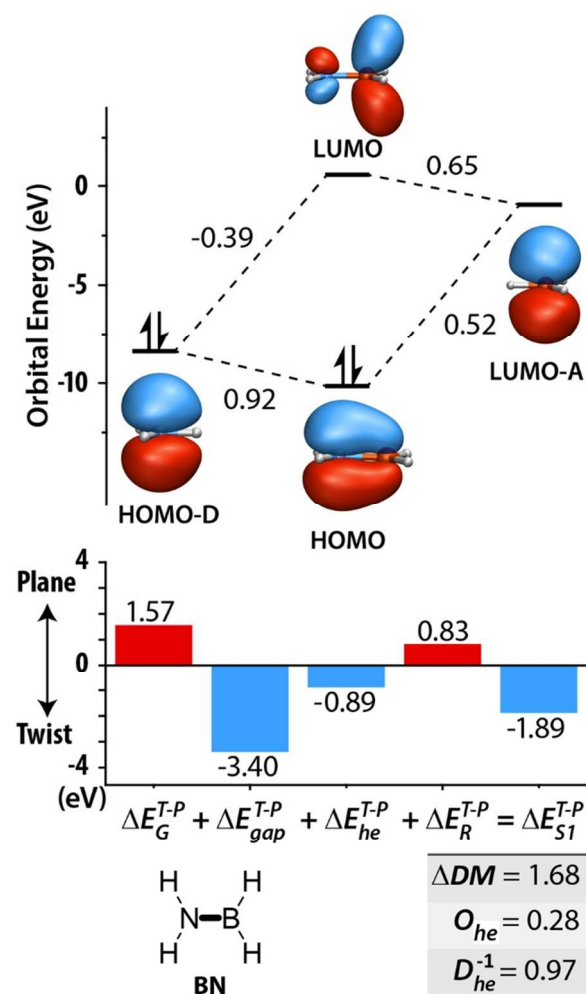


**Figure 1.** Fragmental orbital interaction diagram (top) and excited state energy decomposition chart (bottom) for BN.  $\Delta E_G^{T-P}$  is the ground state energy difference between the planar and twisted ground geometries.  $\Delta E_{gap}^{T-P}$  is the difference in the



energy gap.  $\Delta E_{he}^{T-P}$  is the difference in the hole-electron interaction energy.  $\Delta E_R^{T-P}$  is the difference in the excited state relaxation energy.  $\Delta E_{S1}^{T-P}$  is the difference in the relaxed S1 state energy.  $\Delta DM$  is the difference in the dipole moments of the S1 state, the unit of which is Debye.  $O_{he}$  is the hole-electron overlap in the planar state.  $D_{he}^{-1}$  is the reciprocal of the hole-electron distance in the twisting state, and its unit is  $\text{\AA}^{-1}$ .

The energy decomposition diagram shows that the planar conformation is 1.57 eV more stable than the twisted conformation in the ground state. Additionally, in the first excited state, the twisted state is 1.89 eV more stable, which clearly indicates a TICT state. This result clearly demonstrates that the  $\Delta E_{gap}^{T-P}$  term is the major driving force because the TICT state has a smaller gap, which agrees with the qualitative orbital picture.

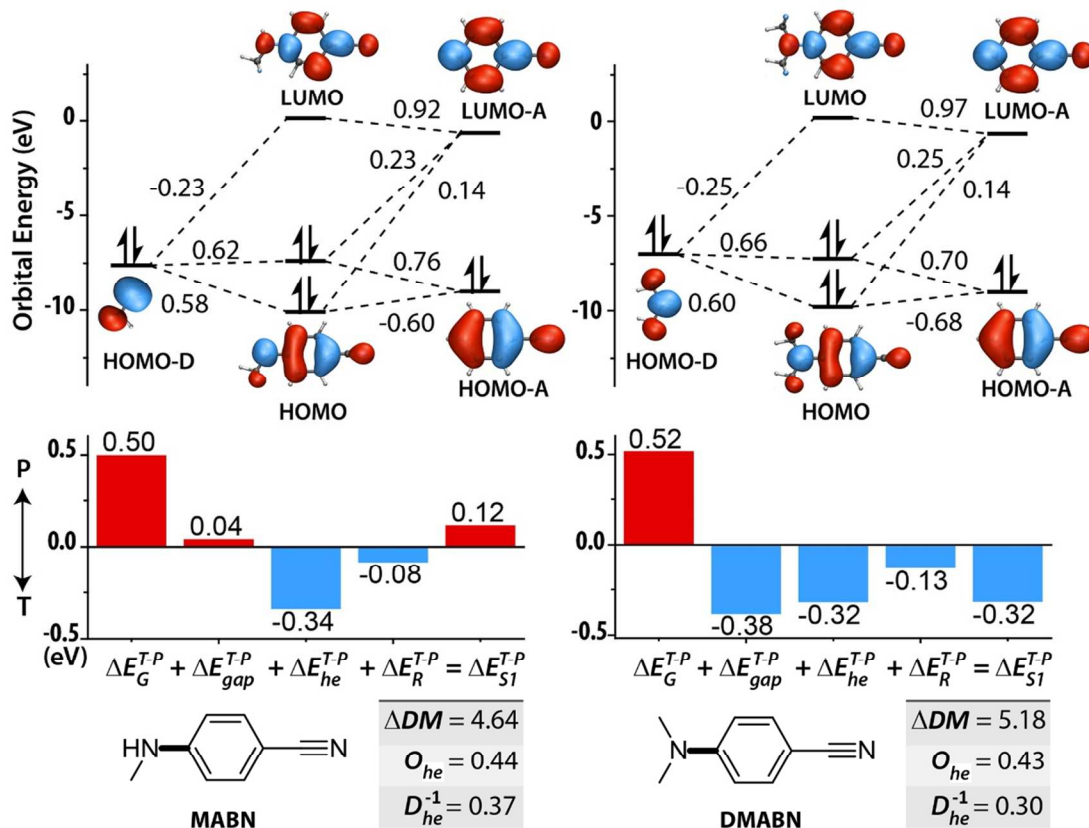


**Figure 2.** Fragmental orbital interaction diagram (top) and excited state energy decomposition chart (bottom) for **MABN** and **DMABN**. See model and computational details for the definitions of all terms.

## II. DMABN and MABN, the effect of donor strength

Now, let us move from the pD-pA case to the pD- $\pi$ A (p donor  $\pi$  acceptor)-type molecule **MABN**. As shown in the left half of Figure 2, the orbital interaction diagram indicates two major differences from the pD-pA case. First, the orbital interactions are weaker because only a small fraction of the acceptor orbital, located on the atom bonded to the donor nitrogen, overlaps with the donor orbital. This interaction decreases the energy difference between the planar and twisted conformations (compare the 0.50 eV conjugation energy of **MABN** to the 1.57 eV conjugation energy of **BN**). Second, the occupied orbital in the acceptor contributes significantly to the HOMO. The HOMO is no longer a bonding orbital but rather is more of a weak antibonding orbital. Therefore, the HOMO-LUMO transition is a weak antibonding to antibonding orbital transition, which is not necessary to twist the bond in the classical sense. This reasoning is confirmed by the driving force decomposition diagram; because the HOMO level is pushed up

by the HOMO orbital of the acceptor (HOMO-A), the resulting  $\Delta E_{gap}^{T-P}$ , 0.04 eV, slightly favors a planar excited state.

While the HOMO-LUMO gap no longer dominates the driving force, another driving force plays an important role in determining the behavior of the pD- $\pi$ A-type molecule: the difference in the hole-electron interactions ( $\Delta E_{he}^{T-P}$ ). The hole-electron interactions, as discussed in part II.a, are influenced by two factors: the overlap of the HOMO and LUMO ( $O_{he}$ ) in the planar conformation and the reciprocal of the hole-electron distance in the twisted conformation ( $D_{he}^{-1}$ ). The hole-electron distance is greater in a twisted excited state, which reduces the hole-electron Coulombic attraction. However, the orbital overlap decreases to nearly zero, which greatly reduces the hole-electron exchange-correlation repulsion. The net effect is that the reduced exchange-correlation repulsion overcomes the reduced Coulombic attraction, which significantly contributes to the formation of the twisted excited state.

The  $\Delta E_R$  term is the difference in the geometry relaxation of the planar and twisted excited states. This term provides a small

contribution to the twisted excited state in pD- $\pi$ A-type molecules. This phenomenon can be explained by the following assumption: in the twisted state, the acceptor only optimizes its structure for the electron, whereas in the planar state, the acceptor may adjust its geometry to stabilize both the electron and hole, which may be less effective. This assumption also holds for the donor.

For **MABN**, the combined hole-electron term and relaxation terms cannot overcome the ground state conjugation energy. The resulting  $\Delta E_{S_1}^{T-P}$  term is smaller than the  $\Delta E_G^{T-P}$  term but still positive, which indicates a PTICT state. Because there were no steric interactions between the D and A, the TICT phenomena could not be observed in **MABN**. In contrast, for the well-known TICT molecule **DMABN**, an addition methyl group on the donor nitrogen increased the donor p orbital level by 0.56 eV relative to the energy level of **MABN**, which decreased the HOMO-LUMO gap in the twisted state by 0.53 eV relative to the energy level of **MABN**. However, the HOMO-LUMO gap in the planar state did not decrease significantly (0.10 eV) because the elevated p level of the donor enhanced its bonding interactions with LUMO-A (LUMO of A group) and reduced its antibonding interactions with HOMO-A, which buffered the increased HOMO level (0.15 eV). In addition, the LUMO level also increased by 0.05 eV due to the elevated p level. Consequently, a relatively large negative  $\Delta E_{gap}^{T-P}$  term was obtained for **DMABN**. This term cannot overcome the ground state conjugation energy alone. However, with the hole-electron term and the relaxation term, the  $\Delta E_{gap}^{T-P}$  term yields a more stable twisted excited state.

### III. 35DCDMA, the effect of the orbital node pattern

**35DCDMA** has the same donor as **DMABN** but a stronger acceptor. **35DCDMA** is more likely than **DMABN** to have a TICT state because of its larger excited state dipole moment. However, no TICT fluorescence has been reported for **35DCDMA**<sup>19</sup>.

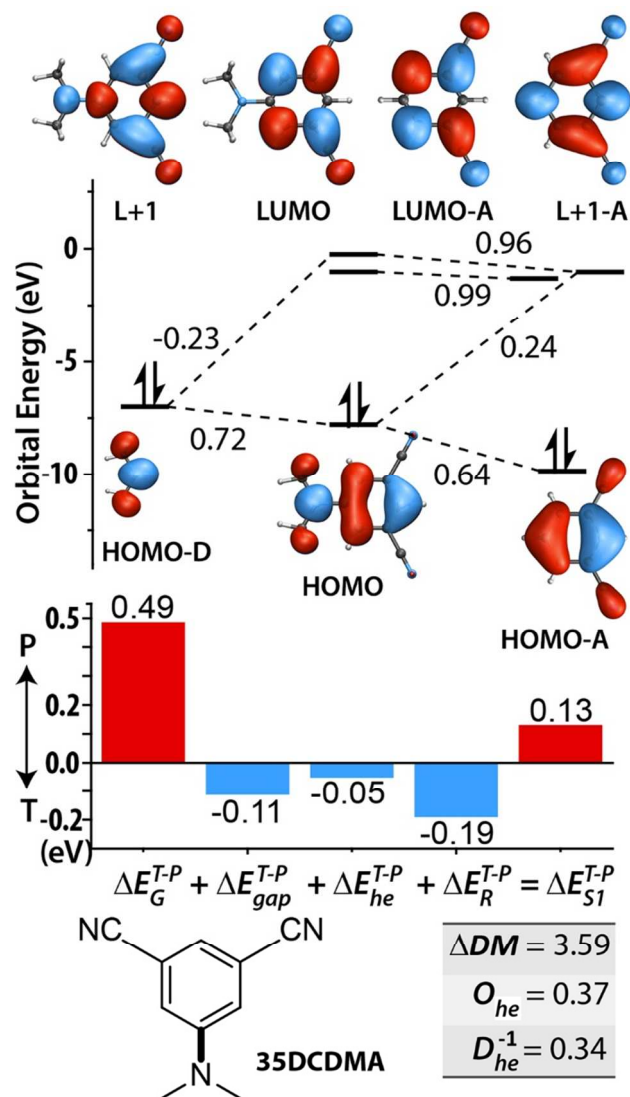


**Figure 3.** Fragmental orbital interaction diagram (top) and excited state energy decomposition chart (bottom) for **35DCDMA**. See model and computational details for the definitions of all terms.

This phenomenon can be interpreted easily using the orbital interaction diagram. The HOMO is a weak antibonding orbital between the donor and acceptor, similar to **DMABN**'s HOMO orbital. However, the LUMO is the same as LUMO-A because LUMO-A has B symmetry in the C<sub>2</sub> point group and cannot interact with the donor orbital. As a result, the HOMO to LUMO transition for **35DCDMA** is a weak antibonding to nonbonding orbital transition, which should not lead to a twisted excited state.

This non-interacting LUMO in the acceptor has two major effects on the energy decomposition diagram. First, LUMO-A and HOMO-A are located at lower energy levels than **DMABN**'s acceptor group, which should yield a more negative  $\Delta E_{gap}^{T-P}$ . However, because the LUMO-A does not interact with the donor orbital, the LUMO level only rises slightly when interacting with the donor orbital (increase of 0.21 eV compared with 0.63 eV for **DMABN**). Therefore, the resultant

$\Delta E_{gap}^{T-P}$  is less negative than that for **DMABN**. Second, because the LUMO orbital is not distributed on the donor or the carbon connected to the donor, the HOMO-LUMO overlap is smaller in the planar state. Therefore, the  $O_{he}$  value is smaller for **35DCDMA** than for **DMABN** (0.37 vs 0.43), which yields a less negative hole-electron interaction term,  $\Delta E_{he}^{T-P}$ . As a brief conclusion, the non-interacting LUMO orbital of the acceptor in **35DCDMA** decreases the driving force for both the orbital gap and the hole-electron attraction, which prevents TICT from being feasible for this molecule.

#### IV. DCS, the effect of acceptor length

What if we increase the acceptor length? The acceptor in **DCS** is approximately twice the length of benzonitrile. According to the literature, this molecule does not exhibit TICT fluorescence for reasons that are not very clear<sup>32, 33</sup>. The orbital interaction diagram in Figure 3 shows that the LUMO level of styrylbenzonitrile (**SBN**) is lower and the HOMO level is higher than those for benzonitrile (**BN**) because of the extended conjugation. As a result, the HOMO and LUMO levels of **SBN** are both closer to the donor p orbital. Thus, one might expect a stronger interaction between these orbitals. This is the case for the HOMO, as demonstrated by the larger coefficient for HOMO-A in **DCS** (0.79 in **DCS** compared with 0.70 in **DMABN**). However, the smaller LUMO-A coefficient (0.14 in **DCS** compared with 0.25 in **DMABN**) indicates a weaker interaction between LUMO-A and the p orbital of the donor. The reason for this weaker interaction is the shape of LUMO-A, which is more heavily distributed on the more electronegative benzonitrile portion. Consequently, the small LUMO-A distribution on the carbon connecting the donor leads to weak interactions between LUMO-A and the donor p orbital. These two effects, the stronger HOMO-A and weaker LUMO-A interactions, give the HOMO of **DCS** an increased antibonding character and thus a higher energy level, and the LUMO of **DCS** has reduced antibonding character and thus a lower energy level. Therefore, the energy gap is smaller for planar **DCS** than for twisted **DCS**, as demonstrated by the large positive  $\Delta E_{gap}^{T-P}$  term. In addition, the  $\Delta E_{he}^{T-P}$  value is less negative because of the large hole-electron distance (small  $D_{he}^{-1}$  value) caused by the elongated acceptor group. The final  $\Delta E_{S_1}^{T-P}$  term is greater than the  $\Delta E_G^{T-P}$  term, which indicates a PICT excited state.

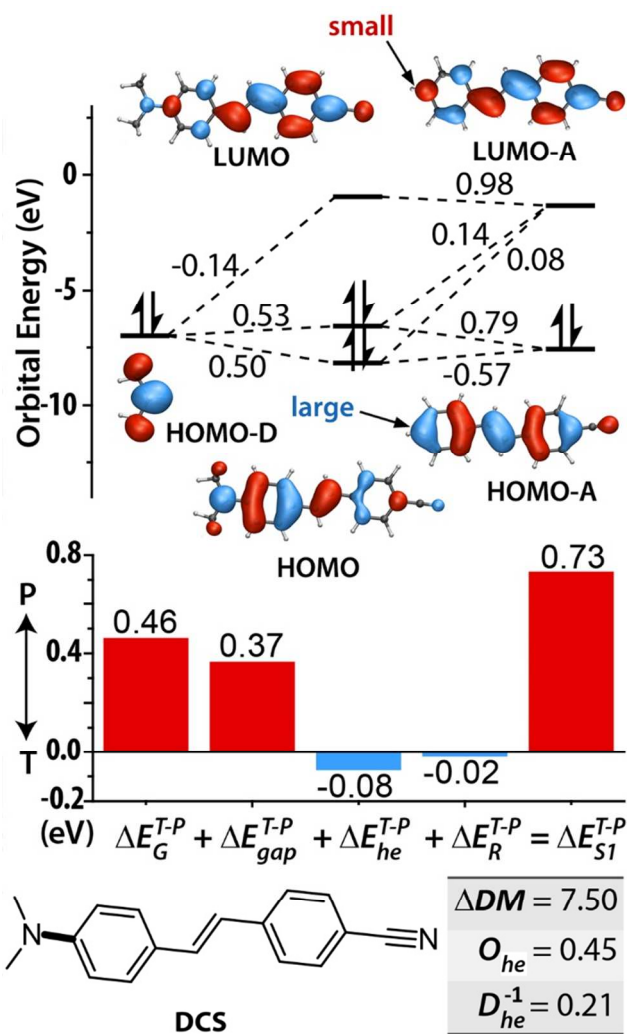


**Figure 4.** Fragmental orbital interaction diagram (top) and excited state energy decomposition chart (bottom) for **DCS**. See model and computational details for the definitions of all terms.

#### V. MP2BN and THT, the effect of $\pi$ donors

The third type of D-A molecule is the  $\pi$ D- $\pi$ A type ( $\pi$  donor- $\pi$  acceptor), as shown in Figure 5. In these molecules, the conjugation energy is smaller than that for molecules of the pD- $\pi$ A type (0.15 eV for **THT** versus 0.52 eV of **DMABN**) because only a small part of the orbitals from both the donor and acceptor can overlap. This trait may lead one to expect that these molecules can be more easily twisted and thus are more likely to form a TICT state. However, another important feature counters this effect. That is, the LUMO of the donor (LUMO-D) can now participate in forming the LUMO for the whole fluorophore. Consequently, the HOMO formed by HOMO-D (HOMO of the donor group) and HOMO-A is usually antibonding and higher in energy than the HOMO of either portion. Additionally, the LUMO formed between LUMO-D and LUMO-A is usually bonding and lower in energy than the

LUMO of either portion, as indicated in **MP2BN**'s orbital interaction diagram. Thus, the HOMO-LUMO transition becomes an antibonding to bonding transition, and  $\Delta E_{gap}^{T-P}$  is now positive. The  $\Delta E_{he}^{T-P}$  term for **MP2BN** is less negative than that for **DMABN** because of the larger hole-electron distance (small  $D_{he}^{-1}$ ). The  $\Delta E_R^{T-P}$  term, despite being approximately the same magnitude as that for **DMABN**, plays a more important role because of the relatively small conjugation energy. For **MP2BN**,  $\Delta E_R^{T-P}$  and  $\Delta E_{he}^{T-P}$  cannot overcome  $\Delta E_{gap}^{T-P}$ , and the resultant  $\Delta E_{ST}$  is slightly greater than  $\Delta E_G$ . Therefore, a PICT state has been observed for **MP2BN**<sup>41</sup>. In our optimization of the excited state geometry, the dihedral angle decreases from 40° in the ground state to 18° in the excited state.

**THT** is another  $\pi$ D- $\pi$ A molecule well known for its fluorescence recovery via DNA binding, the reported

mechanism of which is the suppression of a TICT in the DNA groove<sup>42-44</sup>. **THT** has a much stronger acceptor than **MP2BN**, that is, the HOMO-A and LUMO-A energies are relatively lower. Consequently, LUMO-A and HOMO-D interact more, HOMO-A and HOMO-D interact less, and LUMO-A and LUMO-D interact less. These interactions result in an increased conjugation stabilization energy (0.15 eV compared with 0.08 eV for **MP2BN**). In contrast, the HOMO now has more of a bonding (between HOMO-D and LUMO-A) character and less of an antibonding (between HOMO-D and HOMO-A) character. Similarly, the LUMO now has more of an antibonding character. These traits yield a small, negative  $\Delta E_{gap}^{T-P}$  term for **THT**. The  $\Delta E_R^{T-P}$  and  $\Delta E_{he}^{T-P}$  terms for **THT** overcome the conjugation energy and yield a TICT excited state.

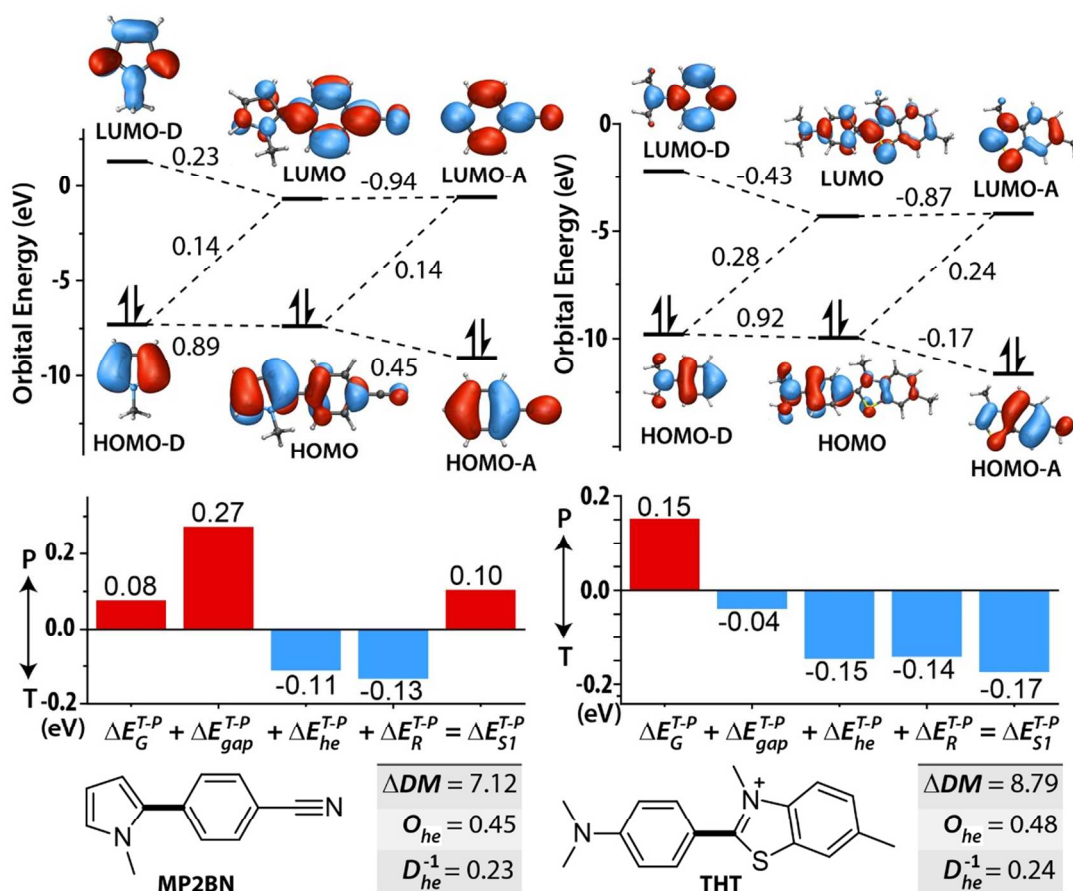


**Figure 5.** Fragmental orbital interaction diagram (top) and excited state energy decomposition chart (bottom) for **MP2BN** and **THT**. See model and computational details for the definitions of all terms.

## VI. DMABN, a note on excited state crossing

The PICT and TICT states for **DMABN** and **BN** differ from those of other molecules studied herein because the transitions corresponding to these two states are composed of different orbitals. The excited state and corresponding orbitals of **DMABN** are shown in Figure 6. By inspecting the transition from the ground state to the FC state, we find that the S1 state is primarily a HOMO – LUMO+1 transition (the reason why S1

is not a HOMO – LUMO transition is because the LUMO and LUMO+1 have very similar energies, but the LUMO+1 overlaps less with the HOMO, which reduces the exchange-correlation repulsion). This state has B symmetry in the C2 group because the HOMO has B symmetry and LUMO+1 has A symmetry. The relaxation of this state decreases the LUMO+1 energy, making it the LUMO in the relaxed B state. Because this orbital is nonbonding (has no distribution on the D), the resultant weak antibonding to nonbonding transition



yields a planar relaxed state. This state is sometimes also called local excited (LE) state because the charge transfer character is weak. Besides, the orbital node in LUMO+1 between the central atoms of the benzene ring yields a so-called AQ (antiquinoid) geometry change (lengthening of the central benzene bonds). The TICT state, on the other hand, originates from the S2 FC state. Formed primarily by the HOMO-LUMO transition, this state has A symmetry in the C2 space group because both of the orbitals involved have B symmetry. The relaxation of this state switches the S1 and S2 states while retaining the LUMO and LUMO+1 orbital order. The orbital distribution on the central bonds of the benzene ring results in a Q (quinoid) geometry change (shortening of the central benzene bonds). Therefore, two local minima with differing electronic structures exist on the S1 surface of **DMABN**.

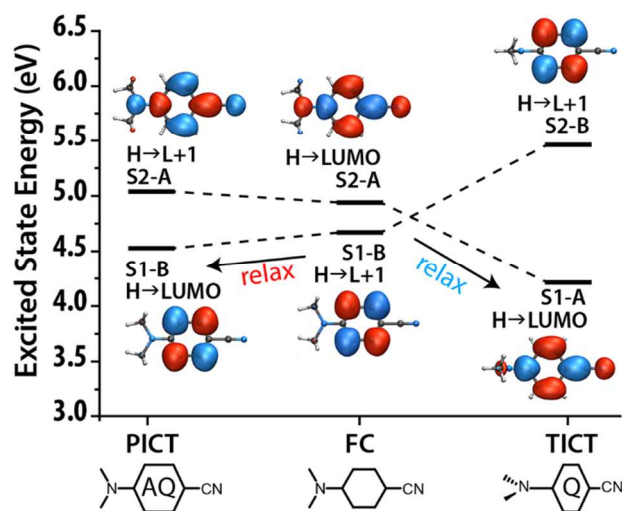


**Figure 6.** Excited state and corresponding orbitals for **DMABN** in its FC, PICT, and TICT states. S1 and S2 refer to the first and second singlet excited states, respectively. The labels A and B refer to the irreducible representations in the C2 symmetry group. Only the orbital graphs for the LUMO and LUMO+1 are shown. See Figure 2 for the orbital graph of the HOMO.

The case of **BN** is a little different from that of **DMABN**. The FC state of **BN** is mainly a HOMO-1 to LUMO+1 transition, while the PICT and TICT states of **BN** are mainly contributed by HOMO to LUMO+1 and HOMO to LUMO, respectively.

The above discussion on excited state crossing has already been elaborated in detail by Andreas Köhn<sup>7</sup> and Yehuda Haas<sup>4</sup> with higher levels of theory. Additionally, this state switching and the two corresponding S1 minima are thought to be necessary for the dual fluorescence of **DMABN**. This conclusion is partly consistent with Zachariasse's PICT theory, which states that the most important condition for ICT to occur is a small energy gap between S1 and S2 in the Franck-Condon region (small energy gap for switching states). However, confusion may exist regarding this point because most theoretical studies examining TICT use **DMABN** or its analogues as examples, which exhibits state switching. Thus, it is easy to assume that state switching is a requirement for TICT

or PICT. However, it should be noted that state switching is not a precondition of either TICT or PICT. Planarization or twisting can occur on S1 state potential energy surfaces regardless of whether the state switches.

## VII. A note on functional selection

We tested various functionals with different Hartree-Fock exchange percentages (BLYP 0% , B3LYP<sup>45</sup> 20% , BHandHLYP<sup>46</sup> 50%, CAM-B3LYP<sup>47</sup> 19%-45%, TDHF, 100%). The calculations performed at the EOM-CCSD/pVDZ level (at cam-B3LYP geometry) were used as references. The resultant  $\Delta E_{S1}^{T-P}$  values are shown in Table 1. Results calculated at the BLYP and B3LYP levels predict TICT states for all the compounds. In contrast, the TDHF level calculation predicts PICT states for all compounds except **BN**. CAM-B3LYP and BHandHLYP, on the other hand, can successfully identify TICT molecules among cases studied in this work. These results agree with the well-known fact that the lower the percentage of HF exchange is, the lower the energy of the CT excited state becomes, which is due to the delocalization error<sup>48-50</sup> of the pure functional. Therefore, functionals with less HF exchange favor the TICT state over PICT state.

CAM-B3LYP predicts the TICT states of **DMABN** in the gas phase, whereas TICT fluorescence cannot be observed for **DMABN** in nonpolar solvents or in vacuum. In this sense, TD-CAM-B3LYP yields an inaccurate result. This may be because that CAM-B3LYP does not have the full 100% asymptotic exchange required in the exchange-correlation potential<sup>51, 52</sup>. This CAM-B3LYP's bias toward TICT state is compensated by the lack of polar solvation model (polar solvation favors the TICT state, so the calculation in vacuum bias toward PICT state), which leads to the successful identification of the TICT molecules in this work; however, the reliability of CAM-B3LYP cannot be guaranteed for other cases because the solvation stabilization energy for TICT or PICT state and the method's bias vary for different molecules. Comparison between CAM-B3LYP and EOM-CCSD indicate that their results have basically the same trend (the TICT molecules, **DMABN** and **THT**, have lower  $\Delta E_{S1}^{T-P}$  values than other compounds), which suggests that the absolute value of  $\Delta E_{S1}^{T-P}$  may not be reliable, and a comparative study including several known compounds is recommended to predict the existence of a TICT state.

**Table 1.**  $\Delta E_{S1}^{T-P}$  values (eV) calculated using various functionals

	BLYP	B3LYP	CAM-B3LYP	BHandHLYP	HF	EOM-CCSD
<b>BN</b>	-2.59	-2.50	-1.89	-2.32	-2.00	-3.03
<b>MABN</b>	-0.78	-0.37	0.12	0.28	0.70	0.49
<b>DMABN</b>	-1.12	-0.80	-0.32	-0.20	0.46	0.11
<b>35DCDMA</b>	-0.59	-0.32	0.13	0.32	0.98	1.62
<b>DCS</b>	-0.34	-0.10	0.73	0.70	0.46	1.16
<b>MP2BN</b>	-0.77	-0.46	0.10	0.09	1.03	0.22
<b>THT</b>	-0.99	-0.67	-0.17	-0.22	0.37	0.16

## Conclusions

### What is the driving force behind TICT?

In addition to the previously established fact that polar solvents stabilize TICT states with large dipole moments, three more factors were proposed here in the framework of molecular orbital theory.

The first and most decisive factor is the energy gap difference between the planar and twisted conformations. For all of the considered molecules, TICT only occurred if the twisted structure had a smaller energy gap than the planar structure. Whether the twisted structure has a smaller energy gap was determined by the HOMO and LUMO features, which will be discussed in detail in part b of the conclusions.

The second factor is the hole-electron interactions of the excited state. Going from planar to twisted conformation, the separation of hole and electron decrease both Coulombic attraction (contributes to PICT) and exchange – correlation repulsion (contributes to TICT). Under most circumstances, the separation distance in twisted state is insufficiently large and there is considerable HOMO-LUMO overlap in planar state, so the exchange – correlation term exceeds the Coulomb term and contributes to TICT. This term contributes less with larger hole-electron distances in the twisted conformation or a smaller HOMO-LUMO overlap in the planar conformation.

The third factor is the geometry relaxation of the excited state. This term usually contributes to the TICT state, which can be intuitively explained by stating that the donor and acceptor structures relax more efficiently for the hole and electron separately in the TICT state than for both carriers simultaneously in the PICT state. This effect usually increases for stronger donors and acceptors and is more notable for  $\pi$ D- $\pi$ A type molecules in which the conjugation energy is small. Although this term may have larger absolute value than the other terms, its variation is usually small for different structures. Therefore, it is not a dominating factor in determining TICT vs PICT.

It is natural to believe that a large ground state conjugation energy (or strong mesomeric interaction) facilitates the formation of a PICT state. However, this is not the case. The large conjugation energy is generally the direct result of strong frontier orbital interaction, specifically, the interaction between HOMO-D and LUMO-A (other orbitals contribute less because of relatively weak interactions caused by larger energy differences). This strong HOMO-D and LUMO-A interaction leads to a large negative  $\Delta E_{gap}^{T-P}$  term, which overcomes the ground state conjugation energy and contributes to the formation of a TICT state. For example, the conjugation energy of **DMABN** is 0.02 eV greater than that of **MABN** due to its stronger donor (higher HOMO-D level), which on the other hand, makes the  $\Delta E_{gap}^{T-P}$  term of **DMABN** 0.42 eV more

negative. The same comparison can also be made for **MP2BN** vs. **THT**.

### Which type of molecule will have a TICT excited state?

The answer to this question depends on the three driving forces described above, with the energy gap being the most decisive factor. Generally speaking, molecules with a smaller energy gap in the twisted state relative to that in the planar state are more likely to have a TICT state. As illustrated in Figure 7, strong HOMO-D and LUMO-A interaction increases the energy gap in planar conformation, which facilitates the formation of a TICT state. In contrast, increasing the HOMO-D and HOMO-A or the LUMO-D and LUMO-A interaction reduces the energy gap in planar state, thus facilitates the PICT state.

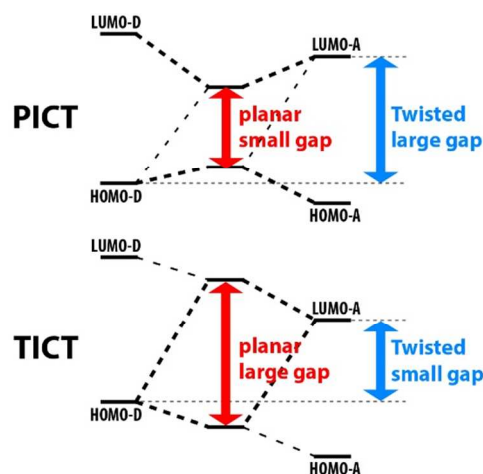


**Figure 7.** Conceptual illustration on how frontier orbitals interactions determine the energy gap of twisted or planar state.

HOMO-D and LUMO-A interact more strongly if they have close energy levels; thus, a higher HOMO-D and lower LUMO-A predict a TICT state. This finding agrees with the widely accepted rule that donors with a low IP (ionization potential) and acceptors with a high EA (electron affinity) facilitate the formation of a TICT state.

HOMO-D and LUMO-A interact more strongly if they have a large spatial overlap, which dictates larger HOMO-D and LUMO-A distributions on the atom connecting the donor and acceptor. The elongation of the acceptor group generally moves the moiety with the strongest accepting ability away from the donor group, which decreases the distribution of LUMO-A and increases the distribution HOMO-A on the bridging atom. In addition, the distance between the hole and electron also increases. These two factors contribute to a PICT state, as shown by **DCS** and other D-A molecules with long acceptor groups.

Sometimes, a node appears on the bridge atom in either HOMO-D or LUMO-A, which not only prevent their interaction but also results in a small HOMO-LUMO overlap in the planar state. Consequently, the TICT state is suppressed, as

evidenced by **35DCDMA**; the two meta-cyano groups keep the LUMO-A distribution off of the bridging atom.

What has not been previously considered, however, are the energy levels of HOMO-A and LUMO-D. Based on the discussion of **DCS** and **MP2BN**, it is clear that an elevated HOMO-A level or reduced LUMO-D level will prevent the formation of a TICT state.  $\pi$ D- $\pi$ A molecules are more likely to have a PICT state than pD- $\pi$ A type because the presence of LUMO-D and LUMO-A interaction, as shown by **DMQA**, **DMABC**, and **4E-PP**<sup>26</sup> (the two  $\pi$  fragments do not twist in the excited state). This is also the reason O-TICT (acceptor rotation, for example, the carbonyl group rotation in **PRODAN**) has rarely been observed because most acceptor groups are of the  $\pi$ A type. Generally, a very strong, even positively charged acceptor group (**DMAPMP**<sup>53</sup>, **THT**) or strong D and A groups with large steric interactions (large ground state twist angle, for example, **MP2B25CN**<sup>41</sup> and **24E-PP**<sup>26</sup>) are required for  $\pi$ D- $\pi$ A molecules to form a TICT state (or, in fact, a PTICT state when the steric interaction is large).

### Acknowledgements

This research was supported by NSFC No. 51203121. We thank Prof. Zhenyang Lin (HKUST Hong Kong) for instruction on MO theory. We thank Sobereva (USTB Beijing) for providing the Multiwfn program and providing instruction on how to run the software. We are also thankful to the High Performance Computing Center of Computer School of Wuhan University.

### Notes and references

<sup>a</sup> Hubei Key Laboratory on Organic and Polymeric Opto-electronic Materials, Wuhan University, Wuhan 430072, China.

Electronic Supplementary Information (ESI) available: All the energy terms needed for the generation of the energy decomposition diagram calculated at the BLYP, B3LYP, BHandHLYP, CAM-B3LYP, HF levels, all transitions and correspond orbitals, all coordinates calculated at the CAM-B3LYP level. See DOI: 10.1039/b000000x/

### REFERENCES

- P. B. Coto, L. Serrano-Andrés, T. Gustavsson, T. Fujiwara and E. C. Lim, *Physical Chemistry Chemical Physics*, 2011, **13**, 15182-15188.
- I. F. Galván, M. E. Martín and M. A. Aguilar, *Journal of Chemical Theory and Computation*, 2010, **6**, 2445-2454.
- Z. R. Grabowski, K. Rotkiewicz and W. Rettig, *Chemical Reviews*, 2003, **103**, 3899-4031.
- S. Cogan, S. Zilberg and Y. Haas, *Journal of the American Chemical Society*, 2006, **128**, 3335-3345.
- S. Murali and W. Rettig, *Journal of Physical Chemistry A*, 2006, **110**, 28-37.
- S. Murali, V. Kharlanov, W. Rettig, A. I. Tolmachev and A. V. Kropachev, *Journal of Physical Chemistry A*, 2005, **109**, 6420-6429.
- C. Hättig, A. Hellweg and A. Köhn, *Journal of the American Chemical Society*, 2006, **128**, 15672-15682.
- M. El-Kemary and W. Rettig, *Physical Chemistry Chemical Physics*, 2003, **5**, 5221-5228.
- A. Pigliucci, E. Vauthey and W. Rettig, *Chemical Physics Letters*, 2009, **469**, 115-120.
- J. S. Yang, K. L. Liao, C. Y. Li and M. Y. Chen, *Journal of the American Chemical Society*, 2007, **129**, 13183-13192.
- J. S. Yang, K. L. Liao, C. M. Wang and C. Y. Hwang, *Journal of the American Chemical Society*, 2004, **126**, 12325-12335.
- A. Samanta, B. K. Paul and N. Guchhait, *Journal of Luminescence*, 2012, **132**, 517-525.
- A. Demeter, S. Druzhinin, M. George, E. Haselbach, J. L. Roulin and K. A. Zachariasse, *Chemical Physics Letters*, 2000, **323**, 351-360.
- K. A. Zachariasse, S. I. Druzhinin, S. A. Kovalenko and T. Senyushkina, *Journal of Chemical Physics*, 2009, **131**.
- K. A. Zachariasse, M. Grobys, T. vonderHaar, A. Hebecker, Y. V. Il'ichev, O. Morawski, I. Rückert and W. Kühnle, *Journal of Photochemistry and Photobiology a-Chemistry*, 1997, **105**, 373-383.
- S. I. Druzhinin, S. A. Kovalenko, T. Senyushkina and K. A. Zachariasse, *Journal of Physical Chemistry A*, 2007, **111**, 12878-12890.
- V. A. Galievsky, S. I. Druzhinin, A. Demeter, P. Mayer, S. A. Kovalenko, T. A. Senyushkina and K. A. Zachariasse, *Journal of Physical Chemistry A*, 2010, **114**, 12622-12638.
- K. A. Zachariasse, S. I. Druzhinin, V. A. Galievsky, A. Demeter, X. Allonas, S. A. Kovalenko and T. A. Senyushkina, *Journal of Physical Chemistry A*, 2010, **114**, 13031-13039.
- K. A. Zachariasse, S. I. Druzhinin, V. A. Galievsky, S. Kovalenko, T. A. Senyushkina, P. Mayer, M. Noltemeyer, M. Boggio-Pasqua and M. A. Robb, *Journal of Physical Chemistry A*, 2009, **113**, 2693-2710.
- S. I. Druzhinin, P. Mayer, D. Stalke, R. von Bülow, M. Noltemeyer and K. A. Zachariasse, *Journal of the American Chemical Society*, 2010, **132**, 7730-7744.
- S. Teichert and K. A. Zachariasse, *Journal of the American Chemical Society*, 2004, **126**, 5593-5600.
- T. Yoshihara, S. I. Druzhinin and K. A. Zachariasse, *Journal of the American Chemical Society*, 2004, **126**, 8535-8539.
- K. A. Zachariasse, S. I. Druzhinin, W. Bosch and R. Machinek, *Journal of the American Chemical Society*, 2004, **126**, 1705-1715.
- M. Dekhtyar, W. Rettig and W. Weigel, *Chemical Physics*, 2008, **344**, 237-250.
- S. Murali and W. Rettig, *Chemical Physics Letters*, 2005, **412**, 135-140.
- W. Weigel, W. Rettig, M. Dekhtyar, C. Modrakowski, M. Beinhoff and A. D. Schlüter, *Journal of Physical Chemistry A*, 2003, **107**, 5941-5947.
- M. Maus and W. Rettig, *Chemical Physics*, 2000, **261**, 323-337.
- M. Maus, W. Rettig, D. Bonafoux and R. Lapouyade, *Journal of Physical Chemistry A*, 1999, **103**, 3388-3401.
- C. A. Guido, B. Mennucci, D. Jacquemin and C. Adamo, *Physical Chemistry Chemical Physics*, 2010, **12**, 8016-8023.
- S. Delmond, J. F. Létard, R. Lapouyade and W. Rettig, *Journal of Photochemistry and Photobiology a-Chemistry*, 1997, **105**, 135-148.
- J. Dobkowski and L. Sazanovich, *Acta Physica Polonica A*, 2007, **112**, S127-S142.
- H. El-Gezawy and W. Rettig, *Chemical Physics*, 2006, **327**, 385-394.
- M. Dekhtyar and W. Rettig, *Journal of Physical Chemistry A*, 2007, **111**, 2035-2039.
- R. Czerwieniec, J. Herbich, A. Kapturkiewicz and J. Nowacki, *Chemical Physics Letters*, 2000, **325**, 589-598.
- R. K. Everett, A. A. Nguyen and C. J. Abelt, *Journal of Physical Chemistry A*, 2010, **114**, 4946-4950.
- H. El-Gezawy, W. Rettig and R. Lapouyade, *Chemical Physics Letters*, 2005, **401**, 140-148.
- H. El-Gezawy, W. Rettig and R. Lapouyade, *Journal of Physical Chemistry A*, 2006, **110**, 67-75.
- G. D. Scholes and G. Rumbles, *Nat Mater*, 2006, **5**, 683-696.
- T. Lu and F. W. Chen, *Journal of Computational Chemistry*, 2012, **33**, 580-592.

40. G. W. T. M. J. Frisch, H. B. Schlegel, G. E. Scuseria, et al., *Gaussian 09, Revision A.02*, (2009) Gaussian Inc., Wallingford CT.
41. S. Murali, P. Changenet-Barret, C. Ley, P. Plaza, W. Rettig, M. M. Martin and R. Lapouyade, *Chemical Physics Letters*, 2005, **411**, 192-197.
42. V. I. Stsiapura, A. A. Maskevich, V. A. Kuzmitsky, K. K. Turoverov and I. M. Kuznetsova, *Journal of Physical Chemistry A*, 2007, **111**, 4829-4835.
43. L. S. Wolfe, M. F. Calabrese, A. Nath, D. V. Blaho, A. D. Miranker and Y. Xiong, *Proceedings of the National Academy of Sciences of the United States of America*, 2010, **107**, 16863-16868.
44. N. Amdursky, Y. Erez and D. Huppert, *Accounts Chem. Res.*, 2012, **45**, 1548-1557.
45. A. D. Becke, *The Journal of Chemical Physics*, 1993, **98**, 5648-5652.
46. A. D. Becke, *The Journal of Chemical Physics*, 1993, **98**, 1372-1377.
47. T. Yanai, D. P. Tew and N. C. Handy, *Chem. Phys. Lett.*, 2004, **393**, 51-57.
48. A. J. Cohen, P. Mori-Sánchez and W. T. Yang, *Science*, 2008, **321**, 792-794.
49. A. J. Cohen, P. Mori-Sánchez and W. T. Yang, *Chemical Reviews*, 2012, **112**, 289-320.
50. A. Dreuw and M. Head-Gordon, *Chemical Reviews*, 2005, **105**, 4009-4037.
51. B. M. Wong and T. H. Hsieh, *Journal of Chemical Theory and Computation*, 2010, **6**, 3704-3712.
52. A. Prlj, B. F. E. Curchod, A. Fabrizio, L. Floryan and C. Corminboeuf, *The Journal of Physical Chemistry Letters*, 2014, **6**, 13-21.
53. V. Kharlanov and W. Rettig, *Chemical Physics*, 2007, **332**, 17-26.